

Remote Sensing Vegetation Hydrological States Using Passive Microwave Measurements

Qilong Min, Bing Lin, and Rui Li

Abstract—A novel technique that links vegetation properties and ET fluxes with a microwave “emissivity difference vegetation index” (EDVI) has been developed and applied to the Amazon region. These EDVI values can be derived from a combination of satellite microwave measurements with visible and infrared observations. This technique is applicable both day and night times under all-weather conditions, which is particularly important for remote sensing since under cloudy conditions classic optical techniques are not applicable. For the Amazon basin, EDVI captures vegetation variation from dense vegetation (rain-forest) to short and/or sparse vegetation (savanna) under all-weather conditions. Good relations between microwave based EDVI and optical indexes of NDVI and EVI are found for various vegetation conditions. More importantly, EDVI shows no sign of saturation even for the tropical rain forest, while NDVI (and EVI to a lesser extent) is clearly saturated. Over the Amazon region in a normal dry season day, EDVI can provide the vegetation information over 98% of the land surface while the optical vegetation indexes can be retrieved only for a small fraction (14%) of the region.

Index Terms—Emissivity difference vegetation index (EDVI), passive microwave, remote sensing, vegetation.

I. INTRODUCTION

THE terrestrial vegetation and ecological systems play important roles in global change and climate variations. An accurate depiction of evapotranspiration (ET) and photosynthesis processes is essential in the understanding of the response and influence of the vegetation system to water, energy, and carbon cycles of the climate. Since clouds have controlling effects on terrestrial carbon uptake [1], it is crucial to monitor vegetation-atmosphere interactions under all weather conditions.

Existing satellite remote sensing techniques for ET, photosynthesis, and vegetation state estimations are generally based on measurements at visible (VIS) and near-infrared (NIR) wavelengths [2]–[6 and references therein], such as normalized

difference vegetation index (NDVI) and enhanced vegetation index (EVI). These spectral measurements are directly related to the absorbed fraction of photosynthetically active radiation (PAR) and have certain correlations with moisture and carbon exchanges of atmosphere and land surface. Another advantage of these indexes is their higher spatial resolutions compared to those at other wavelengths, which is critical in account for the heterogeneity of land surface. The limitations of the measurements are their low temporal resolution caused by high sensitivity to clouds and aerosols (unable to provide information under cloudy conditions) and the saturation at intermediate values of leaf area index (LAI) [7]–[11]. NDVI may represent total vegetation water of leaves when it is not saturated [12]. Because of the rapid change of vegetations during spring onset and fall senescence, these multiday composite indexes cannot accurately capture the transitions of vegetation states during growing seasons. In some regions where cloud covers are high, for example, in the Amazon Basin, these indexes are inadequate in providing information on the structure and function of terrestrial ecosystems, particularly in rain season, while vegetation systems generally have enhanced ET and carbon uptake under cloudy conditions [13], [1]. There are considerable gaps in understanding feedback mechanisms associated with evaporation processes of land surfaces. The wide spectra of spatial and temporal scales of climate system and inherent heterogeneity of the biosphere also require improved remote sensing techniques to study and monitor surface/canopy states, atmospheric and environmental change processes, and the effect of variations in vegetation on atmospheric dynamics and thermodynamics.

There is a long history to use passive microwave measurements for monitoring vegetation and soil properties. Many researches related microwave polarization difference temperature of 37 GHz (MPDT) to soil moisture, surface roughness, canopy structure and vegetation content [14]–[17], as MPDT decreases with increasing vegetation. Justice *et al.* [18] found that MPDT is more sensitive to short vegetation (grass) than to dense vegetation (trees and shrubs). Calvet *et al.* [19] simulated the sensitivity of multiple channel microwave brightness temperature and normalized polarization differences (at 6.6, 10.7, 18, and 37 GHz) to biomass and air temperatures in the boundary layer. They found the biomass effect is better discriminated at lower frequencies. Background soil emission signals can make significant contributions to those vegetation indexes and let the physical explanations difficult. Recently, Shi *et al.* [20] proposed a new microwave vegetation index (MVIs) for short vegetation covers, based on the finding that bare soil emissions at two adjacent frequencies of AMSR-E are highly correlated and can be expressed as a liner function. As pointed out by Prigent *et al.*

Manuscript received February 20, 2009; revised July 23, 2009. First published October 06, 2009; current version published February 24, 2010. This work was supported in part by the Office of Science (BER), in part by the U.S. Department of Energy through the Atmospheric Radiation Measurement (ARM) Grant DE-FG02-03ER63531 and DE-FG02-08ER64559, and in part by the NOAA Educational Partnership Program with Minority Serving Institutions (EPP/MSI) under cooperative agreements NA17AE1625 and NA17AE1623.

Q. Min and R. Li are with the Atmospheric Science Research Center, State University of New York, Albany, NY 12203 USA (e-mail: min@asrc.cestm.albany.edu; rui_li@asrc.cestm.albany.edu).

B. Lin is with the NASA Langley Research Center, Hampton, VA 23681 USA (e-mail: bing.lin@nasa.gov).

Color versions of one or more of the figures in this paper are available online at <http://ieeexplore.ieee.org>.

Digital Object Identifier 10.1109/JSTARS.2009.2032557

[21], atmospheric effects, especially cloud cover, is responsible for a large part of the polarization difference and brightness temperatures, casting doubt on the interpretation of simple indexes solely in terms of surface properties.

To overcome the above limitations, we developed a novel technique that links vegetation properties and ET fluxes with an “emissivity difference vegetation index” (EDVI) [22]–[24]. EDVI is derived from a combination of satellite microwave measurements with visible and infrared observations through accurately atmospheric correction. This technique was demonstrated applicable under all-weather conditions for monitoring vegetation biomass and ecosystem exchange processes in Harvard forest. The characteristics of vegetation in Amazon might differ from those of Harvard forest. As discussed by Min and Lin [22], [23], EDVI is mainly related to the canopy properties of vegetation water content between two effective emission layers. Although the absolute values for a given VWC in the crown layer may be different in Harvard forest and Amazon, the general dependency of VWC should be similar. In order to demonstrate the capability of EDVI technique over large spatial domain for regional and global applications, the technique should be tested in various climate conditions.

The Amazon Basin contains almost one half of the world’s undisturbed tropical evergreen forest as well as large areas of tropical savanna. The forests account for about 10% of the world’s terrestrial primary productivity and the carbon stored in land ecosystems. Furthermore, the Amazon region generally has significant cloudiness although it varies greatly between the wet and dry seasons. As moderate cloudy skies substantially enhance ET and carbon uptake, it is crucial to understand vegetation-atmosphere feedback under all weather conditions [13], [1]. Due to the excessive cloudiness in the region, the classic vegetation indexes from optical sensors may bias or even fail to provide information of vegetation structure and distribution. In this study we applied this technique to the Tropics to illustrate its applicability for various vegetation and weather conditions. We retrieved the EDVI index over the Amazon Basin by mainly combining AMSR-E and MODIS measurements from Aqua for the year 2004.

II. METHOD AND DATASETS

Physical properties of vegetation, such as plant water content, vegetation coverage, canopy structure, vegetation phenology, and physical temperature, are major factors in determining satellite measured radiances ([25]–[27], and references therein). Passive microwave observations have different sensitivities for the dynamic ranges of vegetation structure and biomass from those of visible and infrared measurements, and are less affected by aerosols and clouds [28]. Microwave land surface emissivity (MLSE) can be derived from satellite measurements during both day and night times under all-sky (nonprecipitating) conditions [29]. Thus, a synergism of microwave, infrared, and visible measurements offers great potential to monitor surface and vegetation properties on a continuous basis.

There is a semi-empirical relationship between the optical depth at microwave wavelengths and vegetation water content, which varies systematically with both wavelength and canopy structure [30]. The microwave surface emission above a canopy

is an integration of the microwave radiation from the whole canopy vertical profile and the soil weighted by its transmission. The emissivity observed at longer wavelengths with a weaker attenuation by the canopy generally represents an effectively thicker layer than those observed at shorter wavelengths with stronger attenuation. Thus, we introduce the microwave land surface emissivity difference between two wavelengths to indicate vegetation water content and other vegetation properties of the canopy with a minimal influence of the soil emission underneath vegetation canopy [22], [23]. Analogous to NDVI, the EDVI is defined as

$$\text{EDVI}_p = \frac{\text{MLSE}_p^A - \text{MLSE}_p^B}{0.5(\text{MLSE}_p^A + \text{MLSE}_p^B)} \quad (1)$$

where p represents a polarization at vertical or horizontal direction, and A and B indicate the two wavelengths of microwave measurements. Based on our studies, we chose a pair of channels at about 19 and 37 GHz from current satellite passive microwave sensors as the basic set to investigate their potential for detecting vegetation physiology changes and estimating land-atmosphere exchange. For Special Sensor Microwave/Imager (SSM/I) and Advanced Microwave Scanning Radiometer (AMSR-E), the pair is from measurements at 19.4 and 37.0 GHz and at 18.7 and 36.5 GHz, respectively. The MLSE_p^{19} represents the thicker effective emission layer deeper into the canopy while MLSE_p^{37} represents the thinner one. Thus, EDVI is related to the canopy properties of vegetation water content and structure of two effective emission layers. The studies of Min and Lin [22], [23] found that the EDVI is sensitive to leaf development through vegetation water content of the crown layer of the forest canopy, and demonstrated that the spring onset and growing season duration can be determined accurately from the time series of satellite estimated EDVI within uncertainties of approximately 3 and 7 days for spring onset and growing season duration, respectively, compared to in-situ observations. The leaf growing stage can also be monitored by a normalized EDVI.

All datasets used in this study are summarized in Fig. 1. We retrieved MLSE values of 18.7 and 36.5 GHz from AMSR-E Level 2A Global Swath spatially-resampled brightness temperatures, AE_L2A, using a combined technique [22]. These MLSE values are estimated based on an atmospheric microwave radiative transfer (MWRT) model [31], which accurately accounts for the atmospheric absorption and emission of gases and clouds, especially the temperature and pressure dependences of these radiative properties [32]. The scattering of upwelling microwave radiation is primarily due to precipitation-sized hydrometeors present above the emitting layer [33]–[35]. To avoid the complexity of microwave scattering and the dependence of observed radiances on precipitating hydrometeors, we only processed nonprecipitating pixels identified by AMSR-E product of rain rate/type (AE_Rain). We further filtered out the pixels that Tb85V were less than 285 K to minimize the scattering effects on our retrievals. The information of surface types, i.e., ocean, land, coast, and sea ice, from AE_Rain product are also used to determine validity of pixels for MLSE retrievals: only pixels identified as “land” are included. The

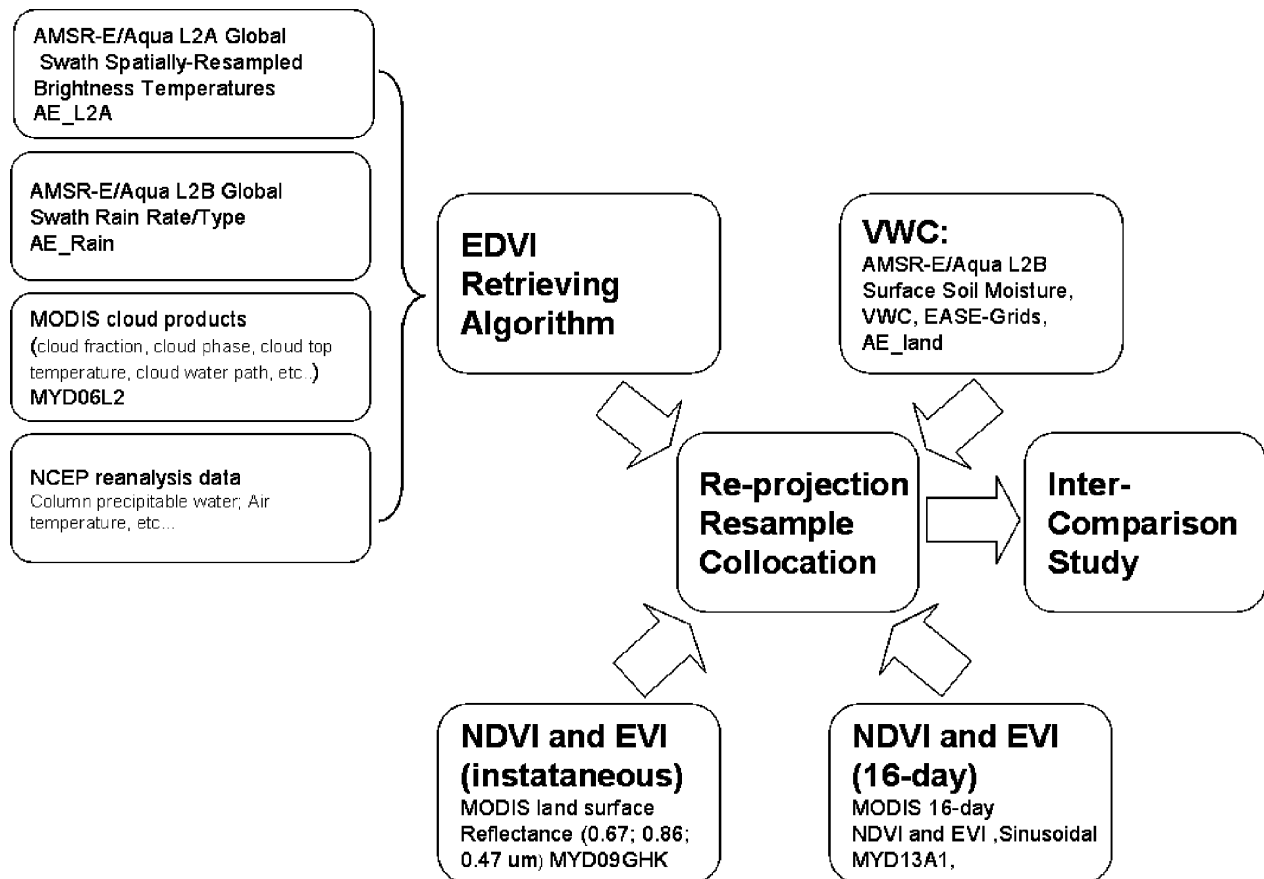


Fig. 1. Summary of all datasets used in EDVI retrieving and in the intercomparison of this study.

major inputs of the model are effective land surface skin temperature, column water vapor (CWV), cloud water amount, surface air temperature and pressure. The NCEP reanalysis data is used to estimate CWV and surface air temperature values. Cloud water amount is adopted from MODIS cloud products (MYD06L2), which are retrieved from combined visible and infrared measurements. Specifically, cloud fraction, cloud phase, cloud top temperature, and cloud water and ice paths are used and projected into AMSR-E spatial grids in the retrievals. The vertical distributions of atmospheric temperature, pressure, and gas abundance are constructed based on climatological profiles [36] and interpolated to conform to the surface temperature and pressure as well as CWV values derived from NCEP reanalysis data. As indicated by the study of Min and Lin [22], [23], the horizontal component of the EDVI is generally more sensitive to a broader range of canopy properties, such as VWC, canopy leaf/stem structure, and orientation, with a larger dynamic range. The crosstalk among these canopy properties may reduce the correlation of the horizontally polarized EDVI with the specific variable evapotranspiration fraction (EF), i.e., evapotranspiration. As shown by Min and Lin [22], the vertical component of the EDVI has a higher correlation with vegetation state and evapotranspiration than the horizontal component. Thus, we used the vertical component of EDVI in the following discussion.

In order to validate and evaluate our retrievals, MODIS land surface reflectance (MYD09GHK) was used to derive instan-

taneous NDVI and EVI under clear-sky conditions. Together with the MODIS standard product of 16-day NDVI and EVI composites (MYD13A1), we projected NDVI and EVI values into the AMSR-E spatial grids for the comparison. We also used AMSR-E retrieved surface VWC and soil moisture (AE_land) for the evaluation [26], [37].

III. RESULTS

Fig. 2 shows retrieved MLSEs at 19 and 37 GHz and derived EDVI based on an Aqua data on August 30, 2004. In the $25^\circ \times 30^\circ$ domain of this case, over 98% of the land surface pixels were valid for MLSE retrievals. In other words, microwave based MLSE and EDVI can provide the vegetation information over 98% of the land surface over the Amazon region. MLSE is indicative of moisture conditions of combined canopy and underneath soil. There is a soil moisture and vegetation gradient from north to south, with low MLSEs at the Amazon basin. Inferred EDVI, which represents vegetation conditions, also clearly shows a gradient from north to south, corresponding to the dense vegetation of rain-forest in the northern Amazon Basin to the savanna in the south. Several high MLSE areas with very low EDVIs are savanna land. In the south-east edge of the image, low EDVIs but relatively low MLSEs indicate sparse vegetation with somewhat moist soils.

Evaluation and validation of retrieved products are keys to the success of a retrieval algorithm. We utilized this case as a basis to assess the uncertainty of our comprehensive retrievals.

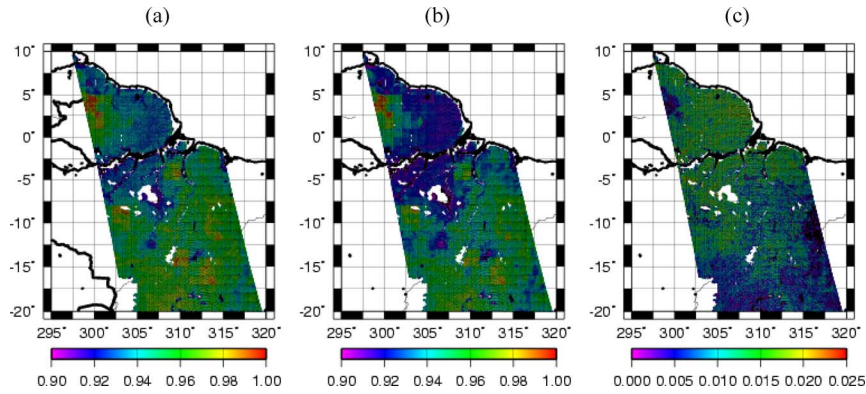


Fig. 2. Retrieved MLSEs at 19 and 37 GHz and derived EDVI over the Amazon Basin on August 30, 2004. (a) Instantaneous MLSE 19. (b) Instantaneous MLSE 37. (c) Instantaneous EDVI.

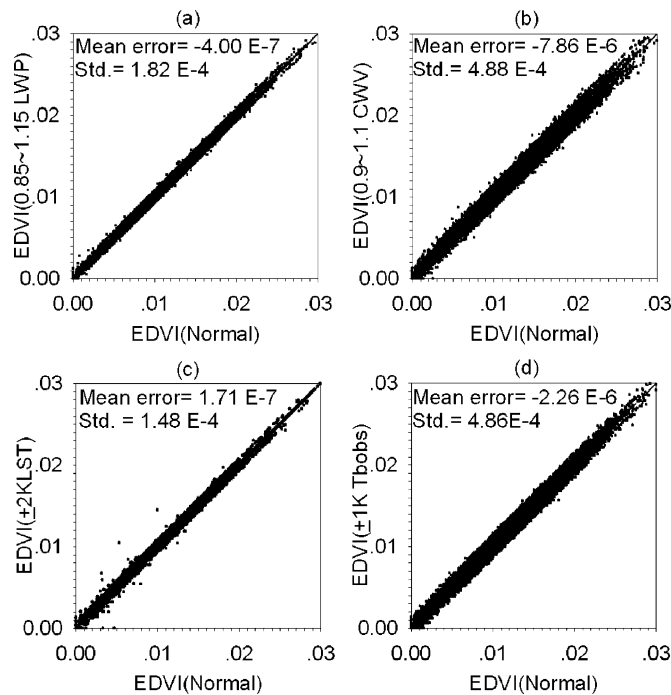


Fig. 3. Comparison between perturbed and normal EDVI with four major error sources. (a) Sensitivity to LWP. (b) Sensitivity to CWV. (c) Sensitivity to LST. (d) Sensitivity to Tbobs.

There are four major error sources that could impact on retrieved EDVIs, including the cloud liquid water path (LWP) retrieved from MODIS, the column water vapor (CWV) estimated from NCEP reanalysis, the land surface skin temperatures (LST) estimated from NCEP reanalysis, and the brightness temperatures (Tb) at 19 and 37 GHz channels observed by AMSR-E. We randomly perturbed each parameter within its maximum uncertainty, based on its measurement or model uncertainty assessment, and compared the perturbed retrievals with the normal retrievals. As shown in Fig. 3, given maximum uncertainties of $\pm 15\%$ in LWP, $\pm 10\%$ in CWV, ± 2 K in LST, and ± 1 K in microwave Tb, respectively, the evaluated standard deviations of EDVI range from $1.48\text{E-}4$ to $4.88\text{E-}4$, i.e., about 1.5% of the averaged EDVI.

To validate our EDVI retrieval, we compared it with optical vegetation indexes of NDVI and EVI as well as VWC retrieved from microwave [37]. Since NDVI and EVI can only be retrieved under clear-sky condition, we compared those indexes in the clear-sky subset of the same Aqua orbit data on August 30, 2004, shown in Fig. 4. In this $25^\circ \times 30^\circ$ domain, the percentage of clear-sky pixels in this normal dry season day is less than 14%. This illustrates that only a small fraction of the land can be monitored by the classic vegetation indexes in the Amazon region. However, over the same domain microwave based EDVI can provide the vegetation information over 98% of the land [Fig. 2(c)].

As shown in Fig. 4(c) and (d), NDVI (and EVI, as well) varies substantially from 0.25 to 0.9, indicating substantial variability of vegetation in the domain, corresponding to the vegetation differences in the north and south. EDVI shows a consistent spatial gradient with NDVI. We further divided the domain into two sectors [see Fig. 4(a)], according to spatial occurrences and vegetation conditions. For all clear-sky pixels, EDVI correlates well with NDVI and EVI in each sector [Fig. 5(a) and (b)]. The slopes between EDVI and NDVI in both sectors are consistent, with statistically significant correlation coefficients of 0.44 and 0.62 for dense vegetation area A and sparse and short vegetation area B, respectively. Slightly better statistic characteristics are evident for EDVI and EVI, due to less saturation of EVI. Overall correlation coefficient in the entire domain is 0.54. Retrieved VWC from microwave measurements has slightly better statistics with NDVI and EVI in the sparse and short vegetation region (area B) than that of EDVI. However, there are almost no correlations between VWC and NDVI (and EVI) in the dense vegetation region (area A). The correlation coefficients between EDVI and VWC are 0.05 and 0.52 in the areas of A and B, respectively. Retrieved VWC may represent integrated VWC for the entire canopy, including branches and trunks [26], while EDVI (and NDVI) represent the upper-most portion of vegetation [23]. It may be one reason for the poor correlations of VWC with other indexes in the dense vegetation region. It is worth noting that although branches and trunks contain most water in the tree, they play a little direct role in the leaf evapotranspiration and photosynthesis processes. Retrieved VWC in the dense vegetation does not represent the vegetation state in terms of atmosphere-land interaction. Nonetheless, these statis-

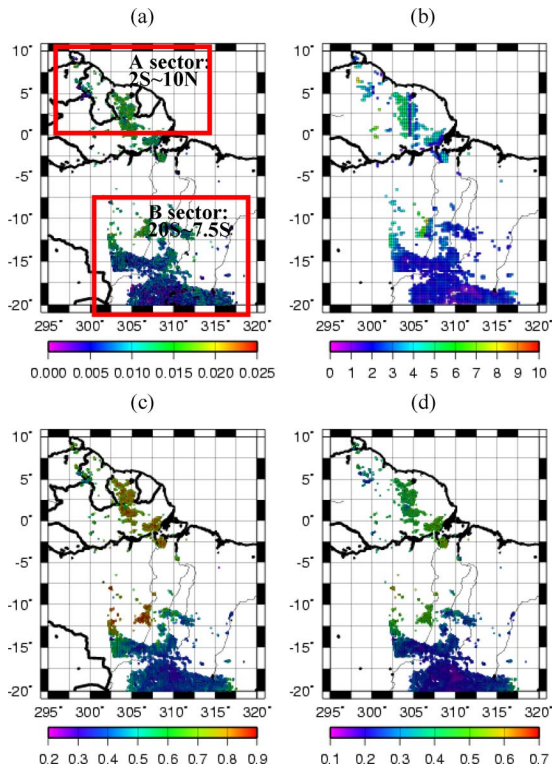


Fig. 4. Comparison among different vegetation indices under clear sky at the Amazon on August 30, 2004: (a) the microwave emissivity difference vegetation index (EDVI); (b) the vegetation water content (VWC) derived from AMSR-E; (c) the normalized difference vegetation index (NDVI); (d) the enhanced vegetation index (EVI).

tics indicate EDVI is applicable to a variety of vegetation conditions for atmosphere-land interactions, much better than VWC in dense vegetation.

Furthermore, as shown in Fig. 6, the histograms of EDVI inside both sectors are close to a Gaussian distribution. The maximum occurrences of EDVI for sectors A and B are at values of about 0.12 and 0.08, respectively. They show no sign of saturation of EDVI even for the densest vegetation in the world, the rainforest of the Amazon Basin. It is worth noting that although the simple two-layer model of Min and Lin [22] shows EDVI saturates at about the VWC value of 0.7 kg/m^2 , it may not reflect real world since the model does not account for multiple scattering effects and only has the first order scattering influences (single scattering). With considerations of full multiple scattering, the increase of EDVI with VWC is going to be slower than what we simulated [22, Fig. 2(b)], and the saturation point of EDVI on VWC should be much higher. On the other hand, the VWC used in the current study is a standard product of AMSR_E, representing the vegetation water content in the entire column (including trunks and branches), however, the EDVI is sensitive to the VWC in the crown layer of the canopy not the entire column of the canopy. From Fig. 6(b), a similar conclusion can be drawn for microwave based retrievals of VWC, which also show similar distributions to the EDVI histograms. In contrast, as shown in Fig. 6(c), the histograms of NDVI illustrate bi-mode distributions. NDVI is clearly saturated with

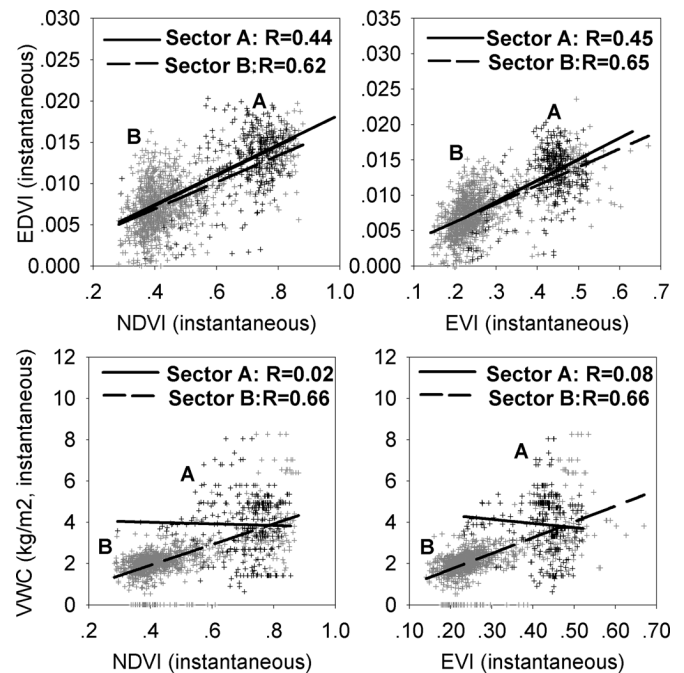


Fig. 5. Comparison among EDVI, VWC, NDVI, and EVI in the north and south sectors under clear-sky conditions on August 30, 2004. (a) Instantaneous EDVI (clear sky); (b) instantaneous VWC (clear sky); (c) instantaneous NDVI (clear sky); (d) instantaneous EVI (clear sky).

distribution skewed to a high value of 0.9. Having similar characteristics to NDVI, EVI exhibits much less problem of saturation than NDVI.

Since optical indexes of NDVI and EVI are not retrievable under cloudy conditions, we further compared instantaneous all-weather EDVI against a 16-day composite NDVI and EVI, shown in Fig. 7. In the figure, we also compared EDVI with VWC. The spatial distribution of instantaneous EDVIs for cloudy pixels corresponds well with the 16-day composites of NDVI and EVI, illustrating EDVI can capture vegetation variation under all-weather conditions.

In order to compare more quantitatively among these indexes, we further divided the region into three sectors based on vegetation characteristics, shown in Fig. 7(a). The sector C is a transition area between dense vegetation area A and relatively short and/or sparse vegetation area (savanna) B. The relationships between EDVI and composite NDVI (EVI as well) for cloudy pixels of ARMS-E are weaker than those from clear-sky instantaneous comparisons, as shown in Fig. 8, because of temporal mismatch and changes of vegetation as a result of the presence of clouds. These relationships get stronger and stronger from dense vegetation to sparse vegetation, due in part to the saturation of optical indexes and sensitivity differences among different vegetation indexes. Note that the relationships between VWC and NDVI (and EVI) are weaker than those between EDVI and NDVI (and EVI), except for sparse vegetation area (sector B). This is consistent with the finding under clear-sky conditions.

A recent study has shown a large seasonal swing in leaf area for Amazon rainforests, which may be critical to the initiation of the transition from dry to wet season and seasonal carbon

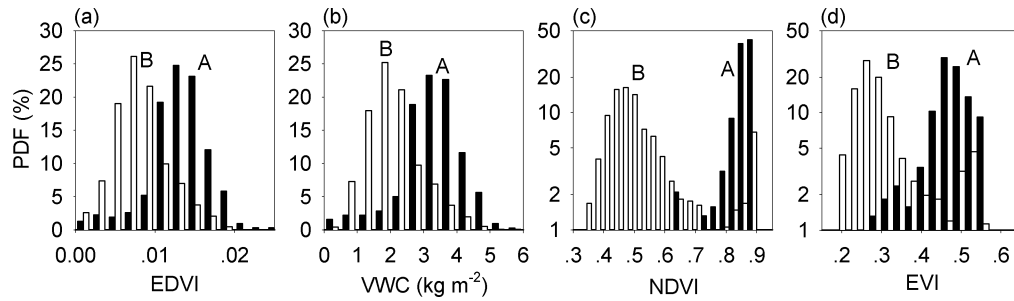


Fig. 6. Histograms of EDVI, VWC, NDVI, and EVI for both A and B sectors.

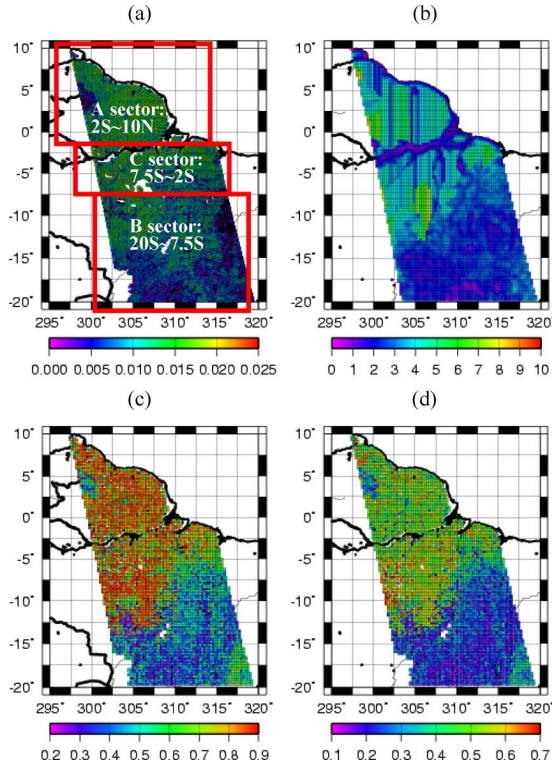


Fig. 7. Comparison among different vegetation indices under all-weather conditions at the Amazon on August 30, 2004: (a) instantaneous EDVI; (b) instantaneous VWC; (c) 16-day composite NDVI; and (d) 16-day composite EVI. (a) Instantaneous EDVI (all sky); (b) instantaneous VWC (all sky); (c) 16-day NDVI (all sky); (d) 16-day EVI (all sky).

balance between photosynthetic gains and respiratory losses in tropical forests [38]. It could have substantial hydrological and biogeochemical significances. As Myneni *et al.* [38] pointed out, it is crucial to minimize the impact of clouds on optical vegetation indexes to monitor seasonal variation of vegetation since there is significant cloudiness in the Amazon region. In contrast to classic vegetation indexes of NDVI and EVI, the EDVI is insensitive to clouds and can be retrieved under both clear-sky and cloudy conditions. Because of the severity of NDVI saturation, we used EVI for the following discussion.

Fig. 9 shows the time series of retrieved EDVI and EVI at one LBA (large-scale biosphere-atmosphere experiment) site of Km67, which is a primary forest. In order to increase temporal samples for EVI, we derived the EVI from reflectances of ten lowest values (500 m resolution of MODIS) within a footprint of AMSR-E ($27 \times 16 \text{ km}^2$), if MODIS cloud mask identifies

these MODIS pixels as clear-sky pixels. For doing so, we allowed EVI to be retrieved under the broken cloud conditions even when the cloud cover in the AMSR-E footprint was up to 99%. For the comparison, we ignored the vegetation variability within the AMSR-E footprint. Even though, the EVI can only be derived by about 27% of all AMSR-E pixels of Aqua overpasses. If we further restrained cloud cover to less than 50% over the AMSR pixels, the retrievable samples of EVI are limited to about 16%, mostly during the dry season. There are some differences of retrieved EVIs with different cloud cover constraints (99% versus 50%), illustrating the inhomogeneous vegetation within the AMSR-E footprint. It is clear, though, that the temporal variations of EDVI (dark solid curve) are consistent with the smoothed variations of instantaneous EVI retrievals with a cloud cover constraint of 99% (light solid curve) at the site, similar to the spatial statistical analysis. Both EDVI and EVI decrease from the wet season to the early dry season and then increase in the late dry season. However, if simply using the 16-day composite EVI data for the Km67 site directly from the MODIS standard product without further screening cloud contamination (dashed curve), the 16-day composite EVI increased slightly from the wet season to the dry season. The different seasonality of short-time scale averages with that of the 16-day composites manifests the issue of cloud impacts on classic optical vegetation indexes and demonstrates the advantage of all-weather measurements of microwave based EDVI. With high temporal resolution, EDVI can monitor vegetation changes even down to the synoptic (a few days) or smaller scales [24], which is critically important for terrestrial hydrological, ecological, and biogeochemical cycling as well as climate modeling. Furthermore, as discussed in Min and Lin [22] and Li *et al.* [24], long term seasonal trend of EDVI is linked to variances of canopy resistance due to the interrelationship among leaf development, environmental condition, and microwave radiation. Short term changes of EDVI caused by synoptic scale weather variations can be used to parameterize the response of vegetation resistance to the quick changes of environmental factors including water vapor deficit, water potential and others. Thus, retrieved EDVI can also be used to estimate evapotranspiration (ET) from the first principle of the surface energy balance model [24].

IV. SUMMARY AND DISCUSSION

Characterization of ET and carbon uptake processes is essential in understanding the responses of climate and terrestrial ecological systems to climate change and variation, which needs advanced remote sensing tools to represent vegetation states. Due

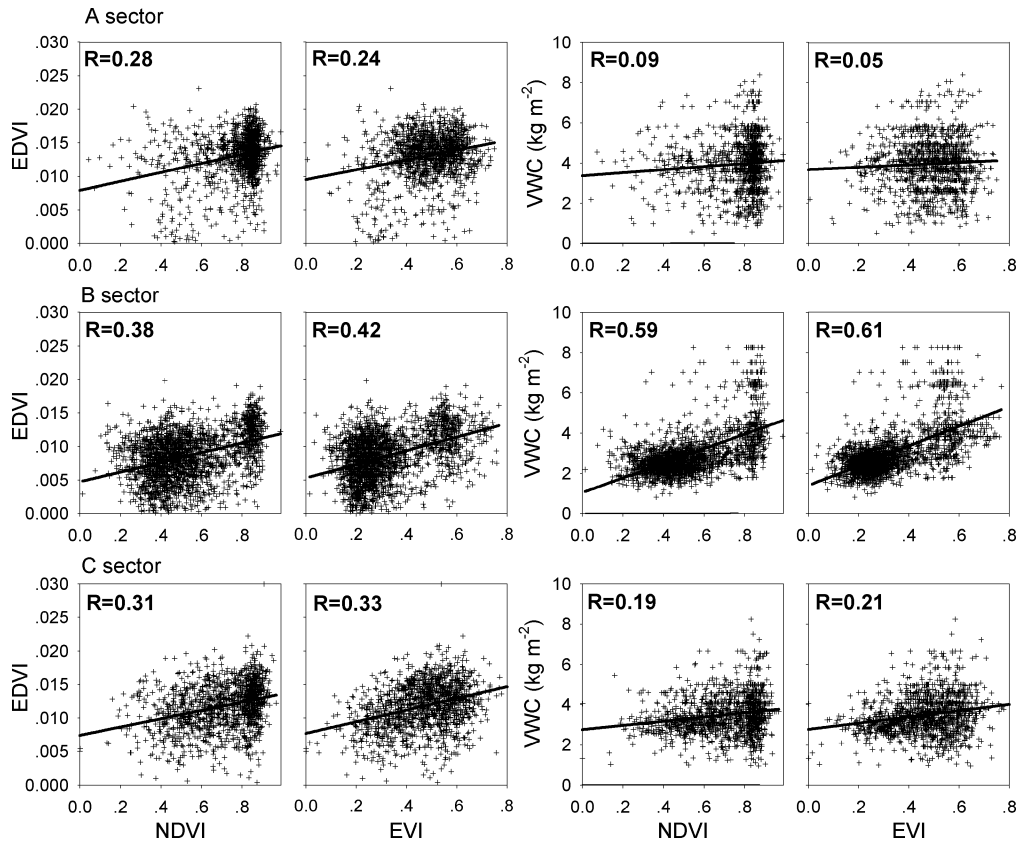


Fig. 8. Comparison of EDVI and VWC with composite NDVI and EVI in three sectors under all-weather conditions on August 30, 2004.

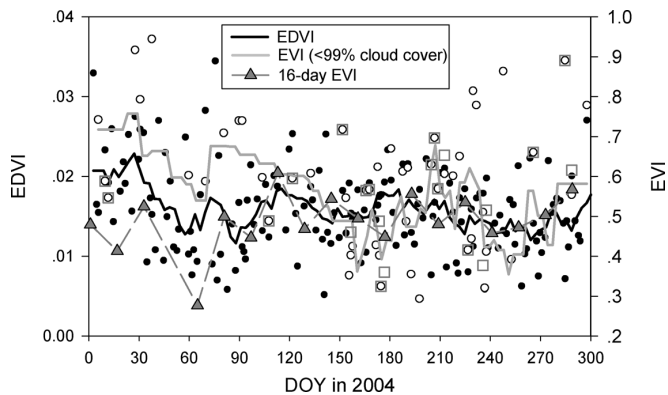


Fig. 9. Time series of EDVI and EVI at an LBA Km67 site. Solid circles represent EDVI; open circles and squares represent EVI with upper limit cloud coverage 99% and 50%, respectively. Solid triangles represent 16-day composite EVI. Black and gray solid curves represent smoothed EDVI and EVI, respectively.

to the limitations of classic optical indexes, we used our newly developed microwave technique [22], [23] to link the “emissivity difference vegetation index” (EDVI) to vegetation properties over the Amazon basin. The EDVI, retrieved from a combination of satellite microwave, visible and infrared measurements, provides an accurate measure of vegetation state under all-weather conditions, where classic optical indexes are unavailable.

At a normal dry season day in the Amazon region, EDVI can provide the vegetation information over 98% of the land sur-

face while the classic vegetation indexes can be obtainable only for a small fraction (14%) of land surface. For a particular footprint of microwave measurements in the Amazon Basin, with the least constraints of cloudy conditions, the frequency of retrievable classic vegetation indexes is only 1/3 of the microwave based EDVI. As illustrated through the intercomparison, EDVI captures vegetation variation from dense vegetation (rain-forest) to short and/or sparse vegetation (savanna) under all-weather conditions. Good relationships between microwave based EDVI and optical indexes of NDVI and EVI are found for various vegetation conditions. More importantly, EDVI shows no sign of saturation even for the tropical rain forest in the Amazon Basin, while NDVI (and EVI to a lesser extent) is clearly saturated. Comparison of microwave based VWC with those indexes indicated that VWC has high correlations with vegetation indexes for sparse vegetation and has no correlation for dense vegetation. Different vegetation indexes may be responsive to different dynamic ranges of vegetation structure and biomass under various sky conditions.

Since the land surface functions as a heterogeneous boundary between the atmosphere and biosphere, the physical, biological and chemical processes related to carbon, energy and water cycles are strongly spatio-temporal scales dependent. This dependence requires observational capability with spatial resolutions from point (surface site or footprint of optical sensor), local (satellite microwave footprint ~ 30 km), and regional to global scales, and with temporal resolutions from minutes for site observations, hours for multiple satellite measurements, to daily

and monthly averages for regional and global composites. Thus, it is extremely useful to generate a unique high spatial and temporal resolution vegetation index by combining high temporal resolution microwave based EDVI with high spatial resolution optical indexes. The synergism product may shed a light on better monitoring and understanding of the exchange processes of land surface and atmosphere.

As a new microwave-related vegetation index, the interpretations of EDVI deserve more detailed studies. The multiple scattering from trees may play an important role in determining the upward microwave signals. And sub-pixel contamination due to open water and wetlands may also introduce additional uncertainties in the EDVI retrievals.

REFERENCES

- [1] Q. Min and S. Wang, "Clouds modulate terrestrial carbon uptake in a midlatitude hardwood forest," *Geophys. Res. Lett.*, vol. 35, no. DOI:10.1029/2007GL032398, p. L02406, 2008.
- [2] R. R. Nemani and S. W. Running, "Testing a theoretical climate-soil-leaf area hydrological equilibrium of forests using satellite data and ecosystem simulation," *Agric. Forest Meteorol.*, vol. 44, pp. 245–260, 1989.
- [3] K. Nishida, R. R. Nemani, S. W. Running, and J. M. Glassy, "An operational remote sensing algorithm of land surface evaporation," *J. Geophys. Res.*, 108(D9), vol. 427, no. DOI:10.1029/2002JD002062, 2003.
- [4] S. W. Running and J. S. Kimball, *Satellite-Based Analysis of Ecological Controls for Land-Surface Evaporation Resistance. Encyclopedia of Hydrological Sciences*, M. G. Anderson and J. J. McDonnell, Eds. New York: Wiley, 2005, vol. 5.
- [5] Q. Mu, M. Zhao, F. A. Heinsch, M. Liu, H. Tian, and S. W. Running, "Evaluating water stress controls on primary production in biogeochemical and remote sensing based models," *J. Geophys. Res.*, vol. 112, p. G01012, 2007.
- [6] E. P. Glenn, A. R. Huete, P. L. Nagler, K. K. Hirschboeck, and B. Paul, "Integrating remote sensing and ground methods to estimate evapotranspiration," *Crit. Rev. Plant Sci.*, vol. 26, pp. 139–168, 2007.
- [7] G. E. Asrar, M. Fuchs, E. T. Kanemasu, and J. L. Hatfield, "Estimating absorbed photosynthetic radiation and leaf area index from spectral reflectance in wheat," *Agron. J.*, vol. 76, pp. 300–306, 1984.
- [8] P. J. Sellers, "Canopy reflectance, photosynthesis, and transpiration," *Int. J. Remote Sens.*, vol. 6, pp. 1335–1372, 1985.
- [9] R. B. Myneni, F. B. Hall, P. J. Sellers, and A. L. Marshak, "The interpretation of spectral vegetation indices," *IEEE Trans. GeoSci. Remote Sens.*, vol. 33, pp. 481–486, 1995.
- [10] G. Gutman, "On the use of long-term global data of land reflectances and vegetation indices derived from the advanced very high resolution radiometer," *J. Geophys. Res.*, vol. 104, pp. 6241–6255, 1999.
- [11] R. J. Granger, "Satellite-derived estimates of evapotranspiration in the Gediz basin," *J. Hydrometeorol.*, vol. 229, pp. 70–76, 2000.
- [12] S. Hong, V. Lakshmi, and E. E. Small, "Relationship between vegetation biophysical properties and surface temperature using multisensor satellite data," *J. Climate*, vol. 20, pp. 5593–5606, 2007.
- [13] Q. Min, "Impacts of aerosols and clouds on CO₂ uptake over Harvard Forest," *J. Geophys. Res.*, vol. 110, no. DOI:10.1029/2004JD004858, p. D06203, 2005.
- [14] B. J. Choudhury and C. J. Tucker, "Monitoring global vegetation using Nimbus-7 37 GHz data: Some empirical relations," *Int. J. Remote Sens.*, vol. 8, no. 7, pp. 1085–1090, 1987.
- [15] F. Becker and B. J. Choudhury, "Relative sensitivity of normalized difference vegetation index (NDVI) and microwave polarization difference index (MPDI) for vegetation and desertification monitoring," *Remote Sens. Environ.*, vol. 24, pp. 297–311, 1988.
- [16] Y. H. Kerr and E. G. Njoku, "A semiempirical model for interpreting microwave emission from semiarid land surfaces as seen from space," *IEEE Trans. Geosci. Remote Sens.*, vol. 28, pp. 384–393, 1990.
- [17] S. Paloscia and P. Pampaloni, "Microwave vegetation indexes for detecting biomass and water conditions of agricultural crops," *Remote Sens. Environ.*, vol. 40, pp. 15–26, 1992.
- [18] C. O. Justice, J. R. G. Townshend, and B. J. Choudhury, "Comparison of AVHRR and SMMR data for monitoring vegetation phenology on a continental scale," *Int. J. Remote Sens.*, vol. 10, no. 10, pp. 1607–1632, 1989.
- [19] J. C. Calvet, J. P. Wigneron, E. Mougin, Y. H. Kerr, and J. L. S. Brito, "Plant water content and temperature of the Amazon forest from satellite microwave radiometry," *IEEE Trans. Geosci. Remote Sens.*, vol. 32, no. 2, pp. 397–408, Feb. 1994.
- [20] J. Shi, T. Jackson, J. Tao, J. Du, R. Bindlish, L. Lu, and S. Chen, "Microwave vegetation indices for short vegetation covers from satellite passive microwave sensor AMSR-E," *Remote Sens. Environ.*, vol. 112, pp. 4285–4300, 2008.
- [21] C. Prigent, F. Aires, W. B. Rossow, and E. Matthews, "Joint characterization of vegetation by satellite observations from visible to microwave wavelength: A sensitivity analysis," *J. Geophys. Res.*, vol. 106, pp. 2373–86, 2000.
- [22] Q. Min and B. Lin, "Remote sensing of evapotranspiration and carbon uptake at Harvard forest," *Remote Sens. Environ.*, vol. 100, pp. 379–387, 2006a.
- [23] Q. Min and B. Lin, "Determination of spring onset and growing season duration using satellite measurements," *Remote Sens. Environ.*, vol. 104, pp. 96–102, 2006b.
- [24] R. Li, Q. Min, and B. Lin, "Estimation of evapotranspiration in a mid-latitude forest using the microwave emissivity difference vegetation index (EDVI)," *Remote Sens. Environ.*, vol. 113, no. DOI:10.1016/j.rse.2009.05.007, pp. 2011–2018, 2009.
- [25] J.-P. Wigneron, J.-C. Calvet, Y. H. Kerr, A. Chanzy, and A. Lopes, "Microwave emission of vegetation: Sensitivity to leaf characteristics," *IEEE Trans. Geosci. Remote Sens.*, vol. 31, pp. 716–726, 1993.
- [26] E. G. Njoku, AMSR Land Surface Parameters, Surface Soil Moisture, Land Surface Temperature, Vegetation Water Content, ATBD of AMSR-E Science Team, NASA EOS Project, 1999.
- [27] J.-P. Wigneron, J.-C. Calvet, T. Pellarin, A. A. Van de Griend, M. Berger, and P. Ferrazzoli, "Retrieving near-surface soil moisture from microwave radiometric observations: current status and future plans," *Remote Sens. Environ.*, vol. 85, pp. 489–506, 2003.
- [28] B. J. Choudhury, Y. H. Kerr, E. G. Njoku, and P. Pampaloni, Eds., *Passive Microwave Remote Sensing of Land-Atmosphere Interaction*, Utrecht, The Netherlands, 1995.
- [29] B. Lin and P. Minnis, "Temporal variations of land surface microwave emissivities over the ARM southern great plains site," *J. Appl. Meteor.*, vol. 39, pp. 1103–1116, 2000.
- [30] T. J. Jackson and T. J. Schmugge, "Vegetation effects on the microwave emission of soils," *Remote Sens. Environ.*, vol. 36, pp. 203–212, 1991.
- [31] B. Lin, B. Wielicki, P. Minnis, and W. B. Rossow, "Estimation of water cloud properties from satellite microwave, infrared, and visible measurements in oceanic environments. I: Microwave brightness temperature simulations," *J. Geophys. Res.*, vol. 103, pp. 3873–3886, 1998.
- [32] B. Lin, P. Minnis, A. Fan, J. Curry, and H. Gerber, "Comparison of cloud liquid water paths derived from in situ and microwave radiometer data taken during the SHEBA/FIREACE," *Geophys. Res. Lett.*, vol. 28, pp. 975–978, 2001.
- [33] B. Lin and W. B. Rossow, "Precipitation water path and rainfall rate estimates over oceans using special sensor microwave imager and International Satellite Cloud Climatology Project data," *J. Geophys. Res.*, vol. 102, pp. 9359–9374, 1997.
- [34] J. Vivekanandan, J. Turk, G. L. Stephens, and V. N. Bringi, "Microwave radiative transfer studies using combined multiparameter radar and radiometer measurements during COHMEX," *J. Appl. Meteorol.*, vol. 29, pp. 561–585, 1990.
- [35] T. T. Wilheit, A. T. C. Chang, J. L. King, E. B. Rodgers, R. A. Nieman, B. M. Krupp, A. S. Milman, J. S. Stratigos, and H. Siddalingaiah, "Microwave radiometric observations near 19.35, 92 and 183 GHz of precipitation in tropical storm cora," *J. Appl. Meteorol.*, vol. 21, pp. 1137–1145, 1982.
- [36] R. A. McClathrey, R. W. Fenn, J. E. A. Selby, F. E. Voltz, and J. S. Garing, *Optical Properties of the Atmosphere*, Air Force Cambridge Res. Lab., 1972, AFCRL-72-0497. Environmental Research Papers, 411.
- [37] E. Njoku, AMSR-E/Aqua L2B Surface Soil Moisture, Ancillary Params, & QC EASE-Grids V002 National Snow and Ice Data Center, Boulder, CO, 2007, digital media.
- [38] Myneni *et al.*, "Large seasonal changes in leaf area of Amazon rainforests," *Proc. Nat. Acad. Sci.*, vol. 104, pp. 4820–4823, 2007.

Qilong Min, photograph and biography not available at the time of publication.

Bing Lin, photograph and biography not available at the time of publication.

Rui Li, photograph and biography not available at the time of publication.